

Structural properties of Fe crystals

W. Zhong, G. Overney, and D. Tománek

*Department of Physics and Astronomy and Center for Fundamental Materials Research,
Michigan State University, East Lansing, Michigan 48824-1116*

(Received 12 June 1992)

We calculate the structural and magnetic properties of iron crystals with body-centered-cubic and face-centered-cubic structures using an approach that combines the tight-binding formalism with the Stoner model of itinerant ferromagnetism. We determine the Slater-Koster parametrization of the tight-binding Hamiltonian using *ab initio* density-functional band-structure calculations for bulk Fe. Our Hamiltonian gives the bcc structure of Fe as the equilibrium phase, and correctly reproduces structural energy differences between bcc and fcc Fe, as well as the stable magnetic states. The predicted lattice constant, cohesive energy, bulk modulus, and magnetic moment are in good agreement with experimental data.

Iron, one of the most important metals, has been the subject of extensive experimental and theoretical research for many years. Its most interesting properties, namely, strong directional bonding and ferromagnetism, make it one of the toughest materials for predictive calculations. Available *ab initio* local spin-density approximation (LSDA) calculations¹⁻³ typically underestimate the lattice constant, and give too large cohesive energies and bulk moduli in comparison to experimental data for Fe.⁴ More important, most of these calculations incorrectly suggest the face-centered-cubic phase to be more stable than the observed body-centered-cubic structure of Fe. This may be indicative of a fundamental deficiency of the LSDA formalism to describe magnetic interactions in bulk Fe with adequate precision.^{1,2}

The importance of iron as a structural material calls for a computationally tractable formalism which not only predicts the correct ground-state equilibrium structure, but which is efficient enough to be used in molecular dynamics calculations of the elastic response at nonzero temperatures. In this paper we develop a formalism which addresses the essential physics in the system without large computational overhead and which can be used in low-symmetry geometries. We show that our Hamiltonian, based on a carefully parametrized tight-binding model which is combined with magnetic interaction terms, can correctly reproduce the equilibrium structure and other structural, elastic, and magnetic properties of Fe.

Our approach is based on the work of Krasko⁵ who combined *ab initio* density-functional calculations with the Stoner theory of itinerant ferromagnetism.⁶ Using this approach, Krasko not only obtained the correct energetics of different iron phases, but also showed that ferromagnetism stabilizes the bcc versus fcc phase of iron. Since the *ab initio* approach cannot handle low-symmetry geometries and large unit cells easily, we decided to develop a sensible parametrization of the band structure instead. Our parametrization is inspired by the previous

success of the one-electron tight-binding Hamiltonian to determine the electronic density of states and magnetic properties of iron.⁷ We expect this formalism to be applicable to a large variety of magnetic materials.

Following Krasko, we separate the total energy of the system into two parts. The first energy contribution is determined by mapping *ab initio* band structures for the solid onto a tight-binding Hamiltonian. In this procedure we keep the essential information about the electronic structure and many-body effects in the system. The second contribution is the magnetic energy of the system, which is evaluated within the Stoner model. We can now write the cohesive energy of the system (with respect to isolated atoms) as a sum of the band structure, repulsive, and magnetic energy, as

$$-E_{\text{coh}} = E_{\text{band}} + E_{\text{rep}} + E_{\text{mag}}. \quad (1)$$

The one-electron band-structure energy is given by

$$E_{\text{band}} = \sum_i \left(\int_{-\infty}^{E_F} E N_i(E) dE - \sum_{\alpha} n_{i,\alpha} \epsilon_{\alpha} \right). \quad (2)$$

Here, the summation extends over all atomic sites i , $N_i(E)$ is the local electronic density of states, and E_F is the Fermi energy which is a global quantity. The reference energy of an isolated atom is expressed in terms of the energy levels ϵ_{α} and the corresponding occupation numbers $n_{i,\alpha}$ which satisfy the condition

$$\sum_{\alpha} n_{i,\alpha} = \int_{-\infty}^{E_F} N_i(E) dE. \quad (3)$$

With this definition, E_{band} is zero for both empty and full bands.

E_{rep} in Eq. (1) is a repulsive interaction. It contains not only the internuclear repulsion, but also all nonmagnetic corrections to E_{band} such as closed-shell repulsion, exchange-correlation, and energy double-counting correc-

tions. We approximate E_{rep} by a sum of pairwise repulsive Born-Mayer potentials, as

$$E_{\text{rep}} = \sum_{i < j} E_r e^{-pr_{ij}}, \quad (4)$$

where E_r and p are constants.

As we mentioned above, the stabilization of the bcc versus fcc phase of Fe is a consequence of the magnetic interaction energy E_{mag} . It is easiest to introduce this energy for a single crystal of fcc or bcc iron, where all the atoms are equivalent, so that $N_i(E) = N(E)$ and $n_{i,\alpha} = n_\alpha$. The magnetic interaction in this system can be obtained using the Stoner theory of itinerant ferromagnetism.⁶ This theory describes the electronic structure of the magnetic system by a rigid shift of the spin-up and spin-down states as

$$\begin{aligned} N_\uparrow(E) &= N(E + \Delta E_\uparrow), \\ N_\downarrow(E) &= N(E - \Delta E_\downarrow). \end{aligned} \quad (5)$$

Here, $N_\uparrow(E)$ and $N_\downarrow(E)$ are the densities of states for spin-up and spin-down electrons corresponding to majority and minority subbands, respectively, and $N(E)$ is the density of states for the nonmagnetic state. The energy shifts ΔE_\uparrow and ΔE_\downarrow of $N_\uparrow(E)$ and $N_\downarrow(E)$ with respect to $N(E)$ are constrained by the charge conservation

$$\int_{E_F - \Delta E_\downarrow}^{E_F} N(E) dE = \int_{E_F}^{E_F + \Delta E_\uparrow} N(E) dE. \quad (6)$$

The total magnetic moment is given by $\mu = m\mu_B$, where m is the number of unpaired electrons and μ_B is the Bohr magneton. m can be obtained by counting the electrons in the spin-up and spin-down subbands, taking care of the charge neutrality given by Eq. (6), as

$$\begin{aligned} m &= \int_{-\infty}^{E_F} [N_\uparrow(E) - N_\downarrow(E)] dE \\ &= \int_{-\infty}^{E_F} [N(E + \Delta E_\uparrow) - N(E - \Delta E_\downarrow)] dE \\ &= 2 \int_{E_F}^{E_F + \Delta E_\uparrow} N(E) dE. \end{aligned} \quad (7)$$

The energy difference between a nonmagnetic and a ferromagnetic state has two parts. The first part is the increase in kinetic energy due to the spin flip of electrons near the Fermi level. The second part is the exchange energy contribution which depends on the Stoner exchange

parameter I . Hence we can write the magnetic energy as

$$E_{\text{mag}} = \int_{E_F - \Delta E_\downarrow}^{E_F + \Delta E_\uparrow} (E - E_F) N(E) dE - \frac{1}{4} I m^2. \quad (8)$$

A self-consistent solution of Eqs. (7) and (8), combined with the stationary requirement $\partial E_{\text{mag}}/\partial m = 0$, is now used to determine the magnetic moment μ and the magnetic energy E_{mag} . The criterion for the occurrence of a stable ferromagnetic state is $IN(E_F) > 1$.

We base our parametrization of the effective one-electron tight-binding Hamiltonian on an *ab initio* calculation of Fe(bcc) and Fe(fcc) crystals using the density functional formalism within the local density approximation.⁸ The LDA formalism has been very successful in predicting the electronic structure of non-magnetic transition metals in agreement with experimental data.⁹ In our calculation we use first-principles pseudopotentials,¹⁰ the Hedin-Lundqvist parametrization of the exchange-correlation potential,¹¹ and a local Gaussian basis. At each site we consider s , p , and d orbitals with four Gaussian decays each, i.e., we represent each Fe atom by 40 totally independent Gaussian orbitals. We use an energy cutoff of 169 Ry in the Fourier expansion of the charge density in order to ensure complete convergence of the LDA spectrum and the total energies. Our results agree very well with previous LDA calculations, but differ from experimental data. We find the calculated lattice constant of Fe(bcc) $a = 2.75 \text{ \AA}$ to be 4% smaller than the observed value $a_{\text{expt}} = 2.87 \text{ \AA}$,¹² and the bulk modulus $B = 262 \text{ GPa}$ to be 56% higher than the experimental value $B_{\text{expt}} = 168 \text{ GPa}$.¹² More important, the LDA calculation energetically favors the fcc versus bcc phase by 0.25 eV per atom.¹³ As mentioned above, these discrepancies are mainly due to the neglect of magnetic interactions which are addressed in E_{mag} .

We find that the cohesion of bulk Fe is mainly due to the hybridization of the localized $3d$ orbitals, whereas the delocalized $4s$ and $4p$ electrons play a less important role. The dominance of localized states suggests that the electronic density of states $N(E)$ of Fe can be described by a tight-binding Hamiltonian. In constructing this Hamiltonian we adopt the parametrization of Slater and Koster.¹⁴ We include $4s$ and $3d$ orbitals only, since the $4p$ orbital lies high above the Fermi level and its limited effect can be modeled by considering a hybrid $4sp$ band. The Slater-Koster parameters are the on-site energies of $4s$ and $3d$ electrons, E_s and E_d , and the hopping integrals $ss\sigma$, $sd\sigma$, $dd\sigma$, $dd\pi$, and $dd\delta$. We consider first and second nearest-neighbor interactions

TABLE I. Slater-Koster tight-binding parameters for Fe. The hopping integrals are listed for the nearest-neighbor distance in bulk Fe(bcc), $r_0 = 2.383 \text{ \AA}$, and obey a power-law distance dependence as $t(r) = t(r_0)(r/r_0)^n$.

	Hopping integrals					On-site energies
	$ss\sigma$	$sd\sigma$	$dd\sigma$	$dd\pi$	$dd\delta$	$E_s - E_d$
Value (eV)	-1.0581	0.6424	-0.6702	0.5760	-0.1445	2.221
Exponent n	2.5	1.8	3.0	4.0	4.0	—

TABLE II. Exchange parameter I and parameters E_r and p of the Born-Mayer repulsive potential for Fe.

I (eV)	E_r (eV)	p
0.632	0.4314	10.00

only, and use a power law for the distance dependence of the corresponding hopping integrals, $t(r) = t(r_0)(r/r_0)^n$. In the mapping procedure from LDA to tight binding, we consider all LDA eigenvalues in the energy range $-\infty < E < E_F + 5$ eV at 14 special k points¹⁵ in the irreducible Brillouin zone of Fe(bcc). The exponent n has been extracted from the LDA results obtained at different lattice constants. The Slater-Koster parameters and their distance dependence are listed in Table I.

As mentioned above, magnetic terms are required in the total energy expression to dilate the lattice, reduce the bulk modulus, and stabilize the bcc phase with respect to the fcc structure. When calculating E_{mag} using Eq. (8), we keep the exchange parameter I constant, i.e., independent of the structure and lattice constant. I is closely linked with the bulk magnetic moment $\mu(\text{bulk})$ and the density of states at the Fermi level. We chose a value of I which closely reproduces the observed magnetic moment in bulk Fe, and which is in fair agreement with the value given in Ref. 5. The calculated value of I is listed in Table II, together with the parameters E_r and p for the repulsive energy E_{rep} .

In Fig. 1 we show the band structure of a Fe(bcc) crystal as obtained using the tight-binding and the *ab initio* LDA method. We find that the agreement between these two calculations is very good, especially in the energy range close to the Fermi level E_F , which is crucial for the magnetic and electronic properties of the solid. Our tight-binding and LDA results for the corresponding total electronic density of states $N(E)$ of Fe(bcc) are displayed in Fig. 2(a), again in very good agreement with each other. The density of states is dominated by a large peak near the Fermi level which is responsible for a stable ferromagnetic phase of Fe(bcc). The corresponding exchange splitting of the spin subbands for this structure is shown in Fig. 2(b).

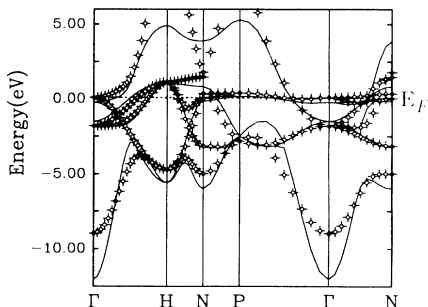


FIG. 1. Band structure of Fe(bcc) obtained using the tight-binding method (solid lines) and LDA (fancy diamonds). The Fermi energy is shown by the dotted line.

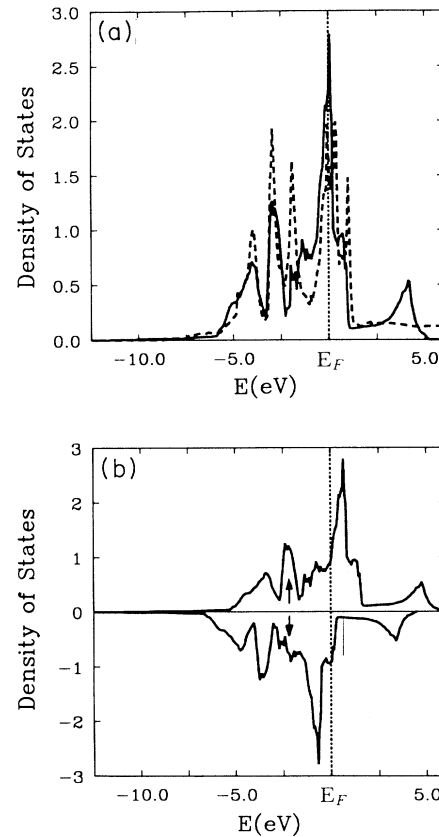


FIG. 2. (a) Nonmagnetic density of states for Fe(bcc) obtained using the tight-binding (solid line) and LDA method (dashed line). (b) Spin density of states for Fe(bcc) using the tight-binding method. The Fermi level is indicated by the dotted line.

The total energy of Fe in the fcc and bcc phases, obtained using Eq. (1), is shown in Fig. 3 as a function of the atomic volume. Our results indicate that the bcc structure is more stable than the fcc structure, in agreement with experiment. We find that the magnetic moments in the stable ferromagnetic phase of Fe(bcc) increase with increasing lattice constant. Fe(fcc), on the other hand, is nonmagnetic near equilibrium, but switches to a ferromagnetic state at large lattice constants. Compared to the fcc phase, the stable bcc phase of Fe has a much smaller bulk modulus. The equilibrium atomic volume of Fe(bcc) is slightly larger than that of the fcc phase, which is mainly due to the lower packing fraction in the bcc structure.

The calculated structural, elastic, and magnetic properties of Fe(bcc) and Fe(fcc) are listed in Table III, together with available experimental data. We find the differences between our results and experimental data for the lattice constant, cohesive energy, and the bulk modulus to be on a few percent level. Much more important is that we correctly determine the bcc phase to be most stable. We also obtain the correct value for the structural energy difference,¹⁸ which will be critical for future molecular dynamics calculations. In Table III we show

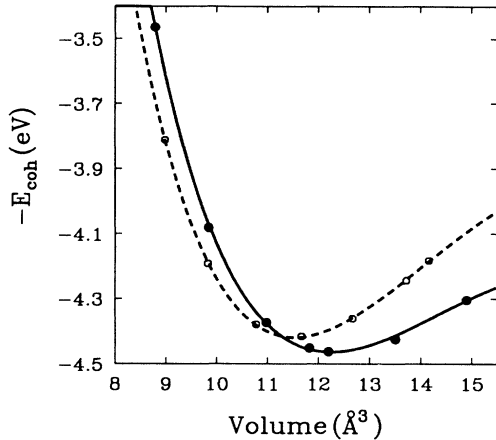


FIG. 3. Cohesive energy of bulk Fe with the bcc (●) and fcc (○) structure as a function of the atomic volume. Solid and dashed lines are cubic polynomial fits to the data points for the bcc and fcc lattices, respectively.

that our Hamiltonian also gives the correct value for the pressure derivative of the bulk modulus, $\partial B/\partial p$, which depends on the third-order derivative of the total energy with respect to the lattice constant. This is a very important quantity which affects quantities such as the melting temperature and the thermal expansion coefficient.

As discussed previously,^{1,2} the local density and spin density functional formalism have failed to determine reliably the structural properties of magnetic materials due to the neglect of long-range correlations. The Stoner model we use here addresses these long-range correlations, and has been successful in determining the ground-state magnetic ordering and magnetic moments in transition metals.⁴ We find that a combination of a one-electron band picture with the Stoner model of itinerant ferromagnetism contains the essential physics governing the cohesion in iron. Our formalism also provides interesting information such as the electronic density of states and the magnetic structure as by-product of the total energy calculation.

The tight-binding Hamiltonian, which we use to describe the electronic structure, correctly addresses the

many-body nature of metallic binding. Unlike the n -body interaction potentials,¹⁹ it describes the resilience of structures to volume and shape deformations by the distance-dependent interatomic interactions and the anisotropy of the intersite hopping integrals. This anisotropy, which is crucial when studying the stability of open phases such as Fe(bcc), is ignored in more simplified techniques such as the embedded atom method (EAM)²⁰ or the many-body alloy (MBA) Hamiltonian.²¹ This is the reason why these techniques typically favor the highly coordinated structures such as the fcc phase.

A very strong advantage of our approach is its computational efficiency. Calculations based on the tight-binding formalism are much easier to perform than analogous *ab initio* calculations. Large unit cells and low-symmetry situations can be handled without many difficulties. Even in the absence of symmetry, the tight-binding Hamiltonian can be used to determine the local density of states from a moment expansion, using the recursion technique.²² In this case, the computational effort in determining the total energy is proportional to the number of atoms N , in contrast to standard total energy calculations based on the diagonalization of a Hamiltonian matrix, which scales as N^3 . We believe that this fact will prove to be a strong advantage when performing molecular dynamics calculations on massively parallel computers.

In conclusion, we have used an approach to calculate the total energy and magnetic properties of Fe, a prototype bulk ferromagnetic. Our calculation is based on a combination of the tight-binding model and the Stoner theory of itinerant ferromagnetism. Our total energy expression addresses the most important aspects pertinent to the cohesion of ferromagnetic materials, namely, the itinerant nature of electrons, anisotropic interactions due to partly filled $3d$ orbitals, and long-range spin correlations. We applied this method to Fe crystals, where previous *ab initio* local density and local spin density calculations have failed to give the bcc phase as the ground-state structure. The results of our calculation for the stable structure, lattice constant, cohesive energy for different structures, bulk modulus, and magnetic ground state are in good agreement with experimental data. Due to its computational efficiency, our method can be ap-

TABLE III. Calculated and observed properties of bulk Fe.

	Lattice constant a (Å)	Cohesive energy E_{coh} (eV)	Bulk modulus B (GPa)	Pressure coeff $\partial B/\partial p$	Magnetic moment μ (μ_B)	Reference
bcc (theory)	2.90	4.46 ^a	165.0	4.78	2.15	This work
	2.76	6.56	240	—	2.06	2
	2.858	—	168.9	7.20 ^b	2.22	17
bcc (expt)	2.87	4.28	168.3		2.22	12
				5.28–5.96		17
fcc (theory)	3.593	4.420	202.4	4.782	0	This work
	3.642	—	231.7	—	0	3

^aReference 16.

^bDerived from Fig. 6 in Ref. 3.

plied easily to extended systems with low symmetry. An implementation of our method to determine structural and elastic properties of magnetic materials at elevated temperatures using molecular dynamics simulations is in progress.²³

We thank K. Hathaway, A. Zangwill, D. A. Papaconstantopoulos, R. Haydock, and T.A. Kaplan for useful discussions and helpful comments. This work has been supported by the Office of Naval Research under Contract No. N00014-90-J-1396.

-
- ¹C.S. Wang, B.M. Klein, and H. Krakauer, *Phys. Rev. Lett.* **54**, 1852 (1985); D. Singh, D.P. Clougherty, J.M. Maclaren, R.C. Albers, and C.S. Wang, *Phys. Rev. B* **44**, 7701 (1991).
- ²K.B. Hathaway, H.J.F. Jansen, and A.J. Freeman, *Phys. Rev. B* **31**, 7603 (1985); H.J.F. Jansen and S.S. Peng, *ibid.* **37**, 2689 (1988).
- ³V.L. Moruzzi, P.M. Marcus, K. Schwarz, and M. Mohn, *Phys. Rev. B* **34**, 1784 (1986).
- ⁴R.O. Jones and O. Gunnarsson, *Rev. Mod. Phys.* **61**, 689 (1990).
- ⁵G.L. Krasko, *Solid State Commun.* **70**, 1099 (1989).
- ⁶E.C. Stoner, *Proc. R. Soc. London, Ser. A* **169**, 339 (1939).
- ⁷F. Liu, M.R. Press, S.N. Khanna, and P. Jena, *Phys. Rev. B* **39**, 6914 (1989).
- ⁸P. Hohenberg and W. Kohn, *Phys. Rev.* **136**, B864 (1964); W. Kohn and L.J. Sham, *Phys. Rev.* **140**, A1133 (1965).
- ⁹J. Callaway and N.H. March, *Solid State Physics* (Academic, New York, 1984), Vol. 38, p. 135.
- ¹⁰D.R. Hamann, M. Schlüter, and C. Chiang, *Phys. Rev. Lett.* **43**, 1494 (1979).
- ¹¹L. Hedin and B.J. Lundqvist, *J. Phys. C* **4**, 2064 (1971).
- ¹²Ch. Kittel, *Introduction to Solid State Physics*, 6th edition (John Wiley, New York, 1986), pp. 23, 55, and 57.
- ¹³This result is in fair agreement with the value E_{coh} (fcc, nonmagnetic) — E_{coh} (bcc, nonmagnetic) = 0.35 eV quoted in Ref. 1. The small difference between the binding energies and lattice parameters obtained using different methods may be due to a different basis, different parametrization of the exchange-correlation potential, and possibly the neglect of core polarization effects in the pseudopotential calculation. Note that our approach does not use LDA total energies for the calculation of structural energies.
- ¹⁴J.C. Slater and G.F. Koster, *Phys. Rev. B* **94**, 1498 (1954).
- ¹⁵D.J. Chadi and M.L. Cohen, *Phys. Rev. B* **8**, 5747 (1973).
- ¹⁶The contributions to the binding energy $E_{\text{coh}} = 4.46$ eV of Fe(bcc), quoted in Table III, are $E_{\text{band}} = -6.20$ eV, $E_{\text{rep}} = 1.91$ eV, and $E_{\text{mag}} = -0.17$ eV.
- ¹⁷*Landolt-Boörnstein* (new series), edited by K.-H. Hellwege (Springer-Verlag, New York, 1979), Vol. III/11, p. 100.
- ¹⁸W. Bendick and W. Pepperhoff, *Acta Metall.* **30**, 679 (1982).
- ¹⁹M.P. Allen and D.J. Tildesley, *Computer Simulation of Liquids* (Oxford, New York, 1990); A.E. Carlsson in *Solid State Physics* (Academic, New York, 1990), Vol. 43, p. 1.
- ²⁰M.S. Daw and M.I. Baskes, *Phys. Rev. B* **29**, 6443 (1984); S.M. Foiles, *ibid.* **32**, 3409 (1985); *Surf. Sci.* **191**, L779 (1987); M.S. Daw, *Phys. Rev. B* **39**, 7441 (1989); S.M. Foiles and J.B. Adams, *ibid.* **40**, 5909 (1989).
- ²¹W. Zhong, Y.S. Li, and D. Tománek, *Phys. Rev. B* **44**, 13 053 (1991).
- ²²R. Haydock, *Solid State Phys.* **35**, 215 (1980); M. J. Kelly, *ibid.* **35**, 295 (1980).
- ²³W. Zhong, G. Overney, and D. Tománek (unpublished).

Errata

**Erratum: Structural properties of Fe crystals
[Phys. Rev. B 47, 95 (1993)]**

W. Zhong, G. Overney, and D. Tománek

Equation (8) in our manuscript should read

$$E_{\text{mag}} = \int_{E_F - \Delta E_1}^{E_F + \Delta E_1} |E - E_F| N(E) dE - \frac{1}{4} I m^2 . \tag{8}$$

All results have been obtained using the correct expression.

0163-1829/93/48(9)/6740(1)/\$06.00

©1993 The American Physical Society

**Erratum: Critical behavior at the extraordinary transition: Temperature singularity
of surface magnetization and order-parameter profile to one-loop order
[Phys. Rev. B 47, 5841 (1993)]**

H. W. Diehl and Martin Smock

Due to a sign error made in the numerical computation of the $d=3$ ($\epsilon=1$) scaling functions $P_{\pm}(\zeta)$, the curves shown in Figs. 1 and 2 are incorrect. Below we provide the corrected Figs. 1 and 2. These extrapolations for $d=3$ were obtained as follows. To ensure that they have the correct short-distance behavior $\sim z^{-\beta/\nu}$, we used the ϵ expansion $P_{\pm}(\zeta, \epsilon) = P_{\pm}(\zeta, \epsilon=0) + \epsilon \partial_{\epsilon} P_{\pm}(\zeta, \epsilon=0) + O(\epsilon^2)$ of our paper to expand the $\ln P_{\pm}(\zeta)$ in $P_{\pm}(\zeta) = \exp[\ln P_{\pm}(\zeta)]$ to order ϵ . Then we set $\epsilon=1$ in the resulting expression $P_{\pm}(\zeta, \epsilon) = P_{\pm}(\zeta, \epsilon=0) \exp\{\epsilon [\partial_{\epsilon} P_{\pm}(\zeta, \epsilon=0)] / P_{\pm}(\zeta, \epsilon=0)\}$. Of course, there are other possibilities of extrapolating to $d=3$. However, for the purpose of seeing whether the profiles decrease in a physically reasonable monotonic fashion, this particularly simple extrapolation method is most convenient.

Further, the following misprints should be corrected.

(a) In Eq. (45a) the factor $\pi/4$ should be replaced by -2π ; i.e., Eq. (45a) should read

$$P_{+}(\zeta) \underset{\zeta \rightarrow \infty}{\approx} 2\sqrt{2} \left\{ 1 + u * \left[\frac{3}{4} + \frac{\ln 2}{2} - 2\pi \left(1 - 2\sqrt{3} + \frac{2\sqrt{3}}{\pi} \ln \frac{2\sqrt{3}+3}{2\sqrt{3}-3} \right) \right] \right\} e^{-\zeta} .$$

(b) In Eq. (39), ξ_{*}^{\pm} means ξ_{\pm}^{*} .

(c) In Eqs. (A7a) and (A7b) the minus sign on the left-hand side should be replaced by a plus sign.

(d) In Eq. (B3), the right-hand side should be multiplied by 8.

(e) In the abstract, "i.e., the extraordinary transition." should be inserted after "... vanishing surface field h_1 ;"

(f) At the end of the first paragraph, "positive-c transition" should be replaced by "ordinary transition".

(g) In Eq. (A5a), $\frac{37}{12}y^4$ should be replaced by $\frac{73}{12}y^4$.

(h) In Eq. (A7b), $\frac{13}{36}y^4$ should be replaced by $\frac{13}{360}y^4$.

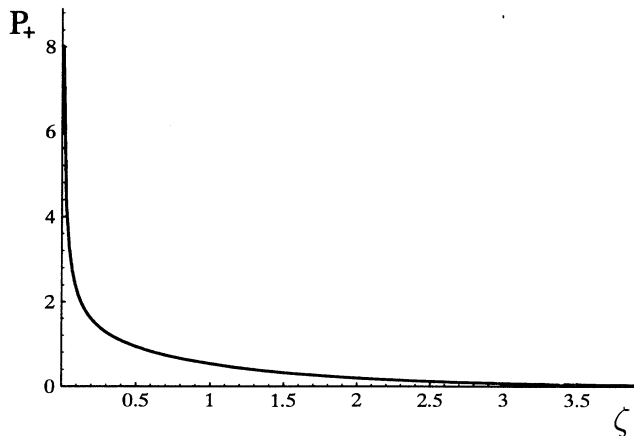


FIG. 1. Scaling function $P_{+}(\zeta)$, with ϵ set to 1, for reduced temperature $\tau > 0$.

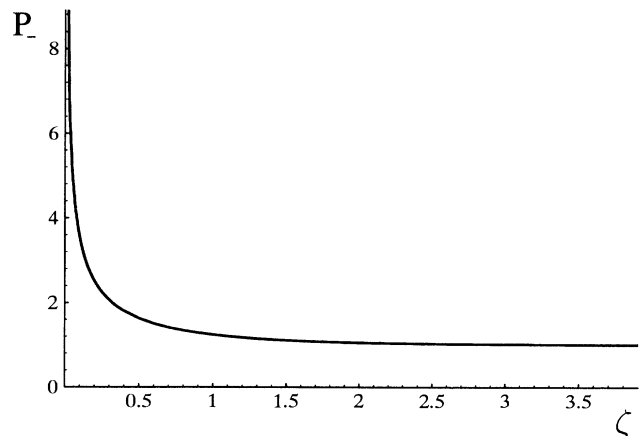


FIG. 2. Scaling function $P_{-}(\zeta)$, with ϵ set to 1, for reduced temperature $\tau < 0$.